

RESEARCH ARTICLE

Advanced handwriting identification: Triboelectric sensor array integrating with deep learning toward high information security

Weiqliang Zhang^{1,2} | Linfeng Deng³ | Xiaozhou Lü¹ | Mingxin Liu¹ |
Zewei Ren⁴ | Sicheng Chen⁵ | Yuanjin Zheng⁵ | Bin Yao¹ | Weimin Bao¹ |
Zhong Lin Wang⁶ 

¹School of Aerospace Science and Technology, Xidian University, Xi'an, China

²National and Local Joint Engineering Research Center for Industrial Friction and Lubrication Technology, Guangzhou, China

³School of Mechanical and Electrical Engineering, Lanzhou University of Technology, Lanzhou, China

⁴School of Advanced Materials and Nanotechnology, Academy of Advanced Interdisciplinary Research, Xidian University, Xi'an, China

⁵School of Electrical and Electronic Engineering, Nanyang Technological University, Singapore, Singapore

⁶Beijing Institute of Nanoenergy and Nanosystems, Chinese Academy of Science, Beijing, China

Correspondence

Zhong Lin Wang, Beijing Institute of Nanoenergy and Nanosystems, Chinese Academy of Science, Beijing 101400, China.

Email: zhong.wang@mse.gatech.edu

Weiqliang Zhang and Xiaozhou Lü, School of Aerospace Science and Technology, Xidian University, Xi'an 710126, China.

Email: wq_zhang@xidian.edu.cn; xzlu@xidian.edu.cn

Funding information

National Natural Science Foundation of China, Grant/Award Numbers: 52105206, 62241308, 92271201; Guangdong Basic and Applied Basic Research Foundation, Grant/Award Number: 2023A1515240050; China Postdoctoral Science Foundation, Grant/Award Number: BX2021230; Opening Project of National and local joint Engineering Research Center for industrial friction and lubrication technology, Grant/Award Number: 2023-GD-0001

Abstract

Handwriting identification is widely accepted as scientific evidence. However, its authenticity is questioned because it depends on the appraiser's professional skills and susceptibility to deliberate false identification by expert witnesses. Consequently, there is an urgent need for an effective handwriting identification system (HWIS) that reduces reliance on the appraiser's skills and mitigates the risk of international false identification. Here, we report a HWIS that integrates a self-powered handwriting signal data acquisition device with an advanced deep learning architecture possessing powerful feature extraction ability and one-class classification function. The device successfully captures the characteristic differences in handwriting behavior between genuine writers and forgers, and the handwriting identification results demonstrate the excellent performance of our system, showcasing its powerful potential to solve the longstanding challenge of handwriting identification that has perplexed humans for a considerable period. Moreover, this work exhibits the system's capability for remote access and downloading the handwriting signal data through the data cloud, highlighting its practical value for fulfilling the requirements of handwriting recognition and identification applications, and it can effectively advance signature information security and ensure the protection of private information.

Weiqliang Zhang and Linfeng Deng contributed equally to this work.

This is an open access article under the terms of the [Creative Commons Attribution](https://creativecommons.org/licenses/by/4.0/) License, which permits use, distribution and reproduction in any medium, provided the original work is properly cited.

© 2025 The Author(s). *InfoMat* published by UESTC and John Wiley & Sons Australia, Ltd.

KEYWORDS

deep learning, handwriting identification, information security, traced handwriting, triboelectric sensor

1 | INTRODUCTION

Handwriting signature is one of the oldest behavioral biometrics and serves as a primary means of communication and information organization. Similar to a human fingerprint, each person's handwriting is characterized by a unique writing style, which exhibits distinct angles and curves. Handwriting identification involves analyzing and comparing handwritten text, such as documents or signatures, to determine their authenticity, authorship, and origin in terms of time and place. This process is typically carried out by specialized examiners who adhere to relevant legal regulations and technical standards, ensuring the accuracy and reliability of their findings. The technology and applications of handwriting identification are extensive and encompass the recognition of handwritten numbers, English letters, Chinese characters, and more. Handwriting-signature is proven highly effective in identifying specific characteristics of an individual, and its utilization is widespread across various fields, including security,¹ forensics, and criminal justice system,² analysis of historical documents,³ and classification of ancient documents.⁴ Advancements in technology have drawn the attention of psychologists, graphologists, forensic experts, and historians, to the analysis of handwriting, which, in some areas of expertise, holds a similar conceptual value as fingerprint systems.⁵⁻⁷ In handwriting recognition, the conventional process begins by converting the mechanical signals into image information and then scanning the characters on paper as digital images for storage and recognition.^{8,9} The scanning process relies on optical methods, and the recognition rate greatly varies depending on factors such as the scanned images' brightness, contrast, and distortion. The two signal conversion processes result in the loss of a substantial amount of original handwritten information, leading to the unreliability of handwriting recognition and authentication.¹⁰ Additionally, deciphering handwritten forms and transforming them into savable and searchable digital media can be time-consuming for record keeping. In pursuit of efficiency, accuracy, and time-saving, mechanical and digital technologies have gradually replaced traditional handwriting methods. Specialized digitizing tablets and pressure-sensitive pens are used to capture a writer's pen movement and dynamic features, including velocity, pressure, and acceleration.^{11,12} Undoubtedly, these dynamic features are unique for individual writers,

resulting in more reliable identification results compared with the traditional methods. However, challenges that arise from the high cost and ongoing efforts to address specific operational requirements, limit the widespread application of these technologies. Consequently, obtaining a comprehensive handwriting identification system (HWIS) that does not rely on the appraiser's professional skills can also mitigate international false identification and remains an ongoing challenge.

In recent years, triboelectric nanogenerators (TENGs), based on the coupling effect of contact electrification and electrostatic induction, have attracted worldwide attraction.¹³⁻¹⁷ The underlying theory of TENGs is rooted in Maxwell's equations, with nanogenerators serving as practical applications of Maxwell's displacement current in energy and sensor technologies.¹⁸⁻²² TENGs offer several advantages, such as low cost, material diversity, simple structure, flexibility, adaptability, and rapid dynamic response, making TENGs an ideal choice for self-powered sensors.²³⁻²⁵ Previous research has shown that the electrical output signal of TENG is directly influenced by external mechanical stimulation and can be utilized for detecting pressure,^{26,27} vibration,^{28,29} velocity,³⁰ position,³¹ and relative displacement.³² Consequently, TENGs were able to serve as promising devices for capturing complex handwriting information without the need for an additional power supply.^{10,12,33,34} In these earlier works, characters were written freely by individuals to record signals from the TENG-based device, which were then processed using various signal processing techniques and recognized through machine learning methods.^{10,35} Furthermore, the electrical output performance of TENGs is directly affected by individual writers,^{36,37} leading to potential instability in long-term use in open environments for handwriting signal recording, which can adversely impact recognition accuracy. Actual cases demonstrated that fraudsters usually forge the handwriting signature by either imitating (placing the handwriting of the genuine writer in front of the eyes and closely observing and copying the handwriting to guarantee the imitated handwriting is close to the genuine writer as much as possible) the genuine writer's handwriting or tracing (overlying the genuine writer's handwriting and tracing it line by line) the signature of the genuine writer to achieve their illegal goals.^{38,39} Therefore, there is a pressing need to develop an anti-humidity handwriting signal acquisition device and

identification system that considers the influence of real-world open environments and practical application scenarios.

With the rapid development of deep learning and triboelectric nanogenerators in the past decade, numerous deep learning and triboelectric nanogenerator-enabled smart systems have been designed to achieve intelligent recognition for complex scenarios.^{40–45} Given the complexity of handwriting information, the utilization of deep learning methods is necessary to accomplish handwriting identification and verification. In this study, we propose a HWIS that integrates a fully packaged triboelectric sensors array for simultaneously capturing handwriting images and digital signals, a deep learning algorithm for extracting the feature information, and a one-class support vector machine (OC-SVM) for handwriting classification. In the development of triboelectric sensors, the FEP and copper film were used as the triboelectric materials, PMMA as the supporting material, and Kapton tape was used as a packaging material. All the materials used are low-cost, commercially available, and suitable for large-scale applications. The device fabrication process is simple and yields devices with excellent output performance and stability. The fully packaged contact-separation triboelectric sensor serves as the base plate, and commercial writing paper is placed on the fully packaged device. When a person writes characters, the handwriting image is obtained and the dynamic writing biometric of the person is reflected in the output signal of the triboelectric sensor. In the meantime, the writer's handwriting signals are recorded. Subsequently, we employ the efficient convolutional neural network (CNN) model, MobileNetV2, to extract the feature information from the handwriting signal. The OC-SVM is utilized as the classifier for the ultimate handwriting classification and identification. Finally, we showcased the physical implementation of the developed system, demonstrating its capabilities in handwriting signal data acquisition, wireless transmission, data uploading to the data cloud, and allocation on multiple display terminals. Additionally, we exhibited the system's capability for remote access through the data cloud and downloading of handwriting signal data, highlighting its practical value for fulfilling the requirements of handwriting recognition and identification applications. The proposed HWIS overcomes the reliance on the appraiser's expertise and the potential bias of expert witnesses in the appraisal process. Therefore, the work addresses the three primary challenges of handwriting identification: (i) the dependence on subjective experience without objective statistical support, (ii) The lack of unified and comprehensive appraisal standards, and (iii) the need for enhanced quality and expertise of professionals. Thus, this work

presents a promising and universal solution for identifying and verifying multilanguage handwriting with high accuracy. It is effectively demonstrated through an experiment validation that proposed HWISs possess the significant potential to solve the longstanding major challenge of handwriting identification that has puzzled customers and researchers for an extended time. In addition, this study proposed uploading and saving handwriting signal data to the cloud, transforming the storage method of handwriting information from the traditional centralized single storage to distributed multiple storage segments, effectively enhancing the security of penmanship information data.

2 | RESULTS AND DISCUSSION

2.1 | Overview of the handwriting identification

Handwriting analysis and identification play an irreplaceable role in various fields and provide crucial support for ensuring the authenticity of documents, maintaining social order, and protecting individual rights. Figure 1 shows the overview of handwriting identification, which encompasses the application scenarios of handwriting identification, common methods used in handwriting analysis and identification, and the proposed handwriting identification method. Handwriting analysis and identification are widely used in daily life, such as being employed in the identification of the authenticity of signatures on authorizations, contracts, legal documents, and financial documents, as shown in Figure 1A. Due to the significant importance of handwriting identification, considerable efforts have been devoted to this field, and several commonly used methods for handwriting identification, including visual comparison, micro-detection, material inspection, and machine learning-based signature image verification, are outlined in Figure 1B. However, current handwriting methods suffer from subjectivity, dependency on individual expertise, variations in technical proficiency, and the impact of handwriting sample quality and clarity on identification results. Here, we propose an advanced HWIS, as shown in Figure 1C. The system incorporates a self-powered handwriting signal acquisition device based on a triboelectric sensor array for capturing the handwriting signals, a deep learning method for extracting feature information, and a one-class support vector machine used as a classifier for identifying and verifying the handwriting of genuine writers and forgers. Traditionally, individuals write characters on paper, and their handwriting is represented as a picture. Therefore, appraisers

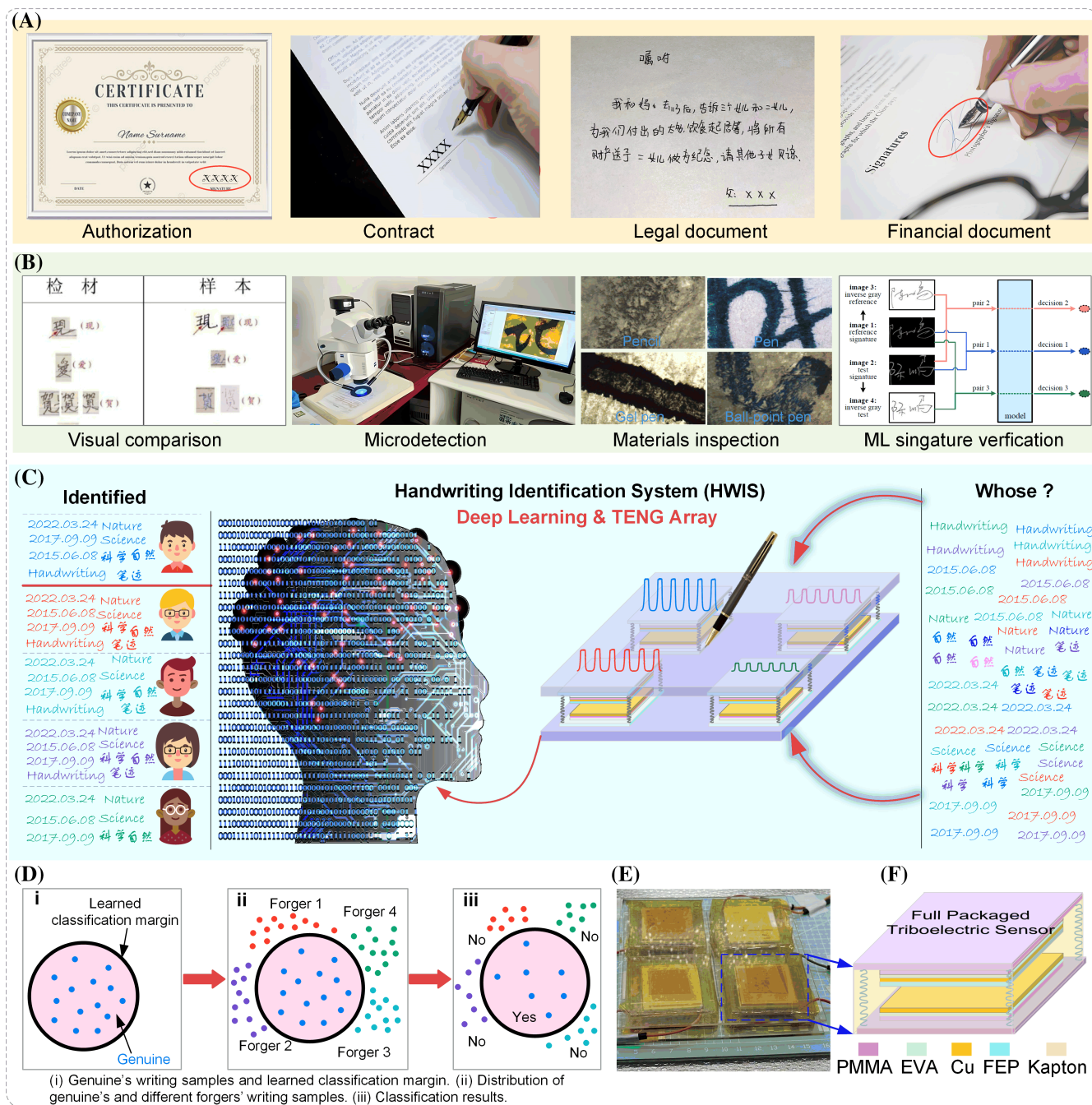


FIGURE 1 Overview of the handwriting identification. (A) Some document types may require signature recognition. (B) Several commonly used methods for handwriting identification. (C) Schematic illustration of the HWIS enabled by the deep learning method and the self-powered handwriting signal acquisition device based on a triboelectric sensor array. (D) Schematic illustration of the classification process of the genuine's and forger's handwriting samples. (E) Physical diagram of the fabricated triboelectric sensor array. (F) Schematic structure of a fully packaged triboelectric sensor cell.

often encounter difficulties when evaluating and verifying handwriting obtained through imitating or tracing the genuine writer. In this system, a self-powered handwriting signal acquisition device based on a triboelectric sensor array serves as a base plate, with commercial paper fixed on its surface. This setup enables the simultaneous acquisition of handwriting images and signals. The

triboelectric sensor array records writing information such as velocity, pressure, and pause, which are reflected in the frequency and amplitude of output signals. The obtained handwriting signals are processed and divided into training data and testing data. The classifier was trained using the training data, and the testing data were input into the trained classifier to classify a person's

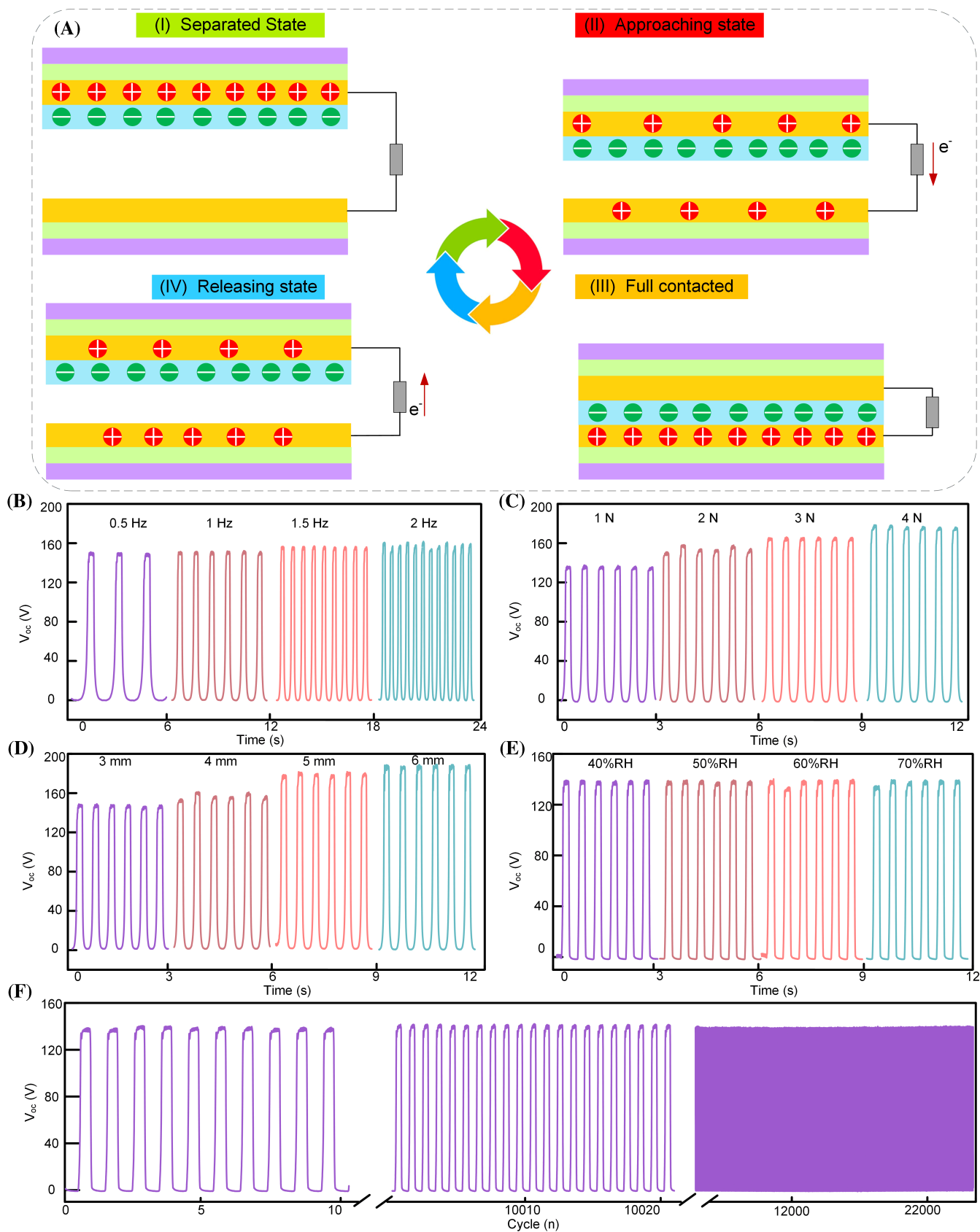


FIGURE 2 Legend on next page.

handwriting. Figure 1D illustrates the classification process of the genuine's and forgers' handwriting samples. Figure 1D(I) shows the genuine handwriting samples and the learned classification hyperplane, Figure 1D(II) displays the distribution pattern of genuine and four different forgers' handwriting samples, and Figure 1D(III) depicts the classification results of handwriting samples that are written by the genuine and any forgers, including the four and all these handwriting samples can only be identified as genuine ("yes", i.e., inside hyperplane) or forger ("no", i.e., outside hyperplane). Figure 1E shows the physical diagram of the triboelectric sensor array. It consists of four fully packaged triboelectric sensors that are evenly distributed on the bottom plate. Figure 1F is the schematic structure of a fully packaged triboelectric sensor cell of the triboelectric sensor array. The electrified FEP is utilized as the top triboelectric layer, and a layer of copper (Cu) film serves as the top electrode. A layer of copper film is employed as the bottom triboelectric layer, with EVA foam used as a buffer layer to enhance the contact area and improve the electrical output performance. PMMA is used as the support, and four springs act as spacers. Finally, the triboelectric sensor is packaged using Kapton film, providing excellent resistance to humidity and dust. This ensures its adaptability to different conditions and guarantees stable output performance.

2.2 | Working principle and fundamental characterization

Taking FEP as the moving part, the working principle of the triboelectric sensor is illustrated in Figure 2A. At the initial state, the top part and bottom part of the triboelectric sensor separate state, negative triboelectric charges are gained by the FEP due to its stronger ability to capture negative charges, whereas the top Cu electrode is left positively charged (I). When the FEP film begins to approach the bottom Cu triboelectric layer, the potential difference between the two surfaces will gradually increase, resulting in an instantaneous electron flow from the top electrode to the bottom electrode in the external circuit (II). This transient flow of electrons continues until the FEP film and bottom Cu electrode are fully contacted (III). When the FEP film begins to separate from the bottom Cu electrode, the potential difference

between the top and bottom Cu electrodes will gradually increase, and the electrons will be repelled back from the bottom Cu electrode to the top Cu electrode through the external load (IV). By repeating the contact-separate process between the top part and the bottom part, an alternative electrical output will be generated. In this study, the amplitude and frequency of the voltage reflect various characteristics of the writers' handwriting behavior features.

The performance of triboelectric sensors relies on crucial parameters such as frequency, force, and contact-separation gap. To investigate their impact on the sensor's performance, systematic experiments were conducted and the results were obtained. The electrified FEP film (with a size of 35×35 mm) was used as the moving part, driven by a linear motor to periodically contact and separate with a commercial copper film (with a size of 35×35 mm) was used as the bottom and triboelectric layer that was mounted on a three-coordinate displacement plate. The frequency-dependent output electrical signals were examined under a gap of 4 mm and a driving force of 2 N. Figure 2B shows the open-circuit voltage of the device at different frequencies from 0.5 to 2 Hz and the voltage maintained nearly constant values of ~ 150 V. The transfer charges (Q) of the device at different frequencies in the range from 0.5 to 2 Hz exhibited the same trend (Figure S1A). This observation suggests that equal triboelectric charges were generated on the triboelectrification layer, resulting in the same amount of static charges on both electrodes. Consequently, the transfer charges and potential difference between the electrodes remained constant. However, the peak-to-peak value of short-circuit current (I_{sc}) increased from 2.5 to 7 μ A with the increase in frequency indicating an elevated rate of electron transfer (Figure S1B). The output electrical signals under different driving forces were carried out under a frequency of 2 Hz and a gap of 4 mm. Figure 2C illustrates the open-circuit voltage signal of the device as the driving force gradually increases from 1 to 4 N. It can be observed that with the increase in driving force, the open-circuit voltage shows a progressively increasing trend. The short-circuit current and transfer charges (Q) exhibit the same trend with the driving force increase from 1 to 4 N (Figure S1C,D). Notably, the device exhibited higher sensitivity at a force of 1 N. Considering the variation in writing pressure among different individuals, the device's ability to capture

FIGURE 2 Working principle and fundamental characterization of the triboelectric sensor. (A) Working principle of the triboelectric sensor. (B) The open-circuit voltage at various frequencies. (C) The open-circuit voltage under different driving forces. (D) The open-circuit voltage under different contacting-separating distances. (E) The open-circuit voltage of the fully packaged triboelectric sensor under different relative humidity levels. (F) The stability and durability testing of the fully packaged triboelectric sensor.

handwriting signals was further validated by measuring its performance under lower normal force. Remarkably, the device was able to generate a 5 V output even under a normal load of just 0.05 N (Figure S1E). The output electrical signals under different contact-separation distances were carried out under a frequency of 2 Hz and a driving force of 2 N. Figure 2D displays the open-circuit voltage of the device at different gap distances. It was found that, as the separation distance increases from 3 to 6 mm, the open-circuit voltage increases from ~ 150 V to around 190 V. The short-circuit current and transfer charges (Q) remain essentially stable (Figure S1F,G); this may be because the charge reaches saturation at a separation distance of 3 mm. The contact area between the triboelectric sensor's upper and lower triboelectrification layers varies with the writing pressure. The output performance of devices with different areas was tested under a driving force of 2 N and a frequency of 2 Hz. As the device area decreases, the output performance declines, but a device with an area of 1×1 cm still generates an output voltage of over 10 V (Figure S2). Figure 2E shows the electrical performance of the fully packaged triboelectric sensor under different relative humidity levels at a driving force of 2 N and a frequency of 2 Hz. As we know, humidity has a detrimental effect on the electrical output performance of triboelectric sensors due to the dissipation of triboelectric charges in a high-humidity environment. However, the packaging approach employed in this study effectively eliminated the impact of humidity on the triboelectric sensors. Consequently, the electrical output performance, including V_{oc} , I_{sc} , and Q , exhibited good stability even as the relative humidity increased from 40% to 70%. Additionally, the packing approach offered the added advantage of protecting the triboelectric sensors from the effects of dust in the operating environment. It was expected that the electrical output performance of every triboelectric sensor cell in the array would be consistent so that the differences in writing behavior could be well captured. The electrical output performance of the four fully packaged triboelectric sensors under a condition of a driving force of 2 N and a frequency of 2 Hz (Figure S3). It was evident that there were minor variations in V_{oc} , I_{sc} , and Q among the four triboelectric sensors, indicating good overall consistency. However, it should be noted that there were some performances between packaged and unpackaged triboelectric sensors. This disparity could be attributed to the presence of a prestressing force that occurred during the encapsulation process using Kapton film. The durability of the device was crucial for practical application, and the durability of the triboelectric sensor was evaluated, as shown in Figure 2F. The results demonstrated that the triboelectric sensor maintained a stable electrical performance

even after 25 000 continuous cycles under a driving force of 2 N and a frequency of 2 Hz. This indicated that the developed self-powered handwriting recording device consisting of a triboelectric sensor array was adapting to varying humidity levels in a practical application environment and could operate over an extended period.

2.3 | Handwriting images and signals

Traced and imitated handwriting signatures were commonly used in signature theft and could be challenging to identify accurately. Traditionally, characters were recorded on paper; only the static features of the handwriting signature were stored as grayscale or binary images while disregarding the dynamic writing information. Given that English, Chinese, and numerical characters were extensively used worldwide, their identification and verification were crucial for information security. In this study, Mr. Liu is the genuine writer, while Miss Ma, Mr. Sun, Mr. Wang, and Miss Wang played the role of the forgers. Tracing is another common method of handwriting forgery. The handwriting images and signals were obtained by writing on the commercial writing papers fixed on the designed device. The process of obtaining handwriting from the genuine writer and the traced handwriting from forgers was shown in Movie S1. Figure 3 shows the representative handwriting images and signals of the genuine writer and the representative traced handwriting images and signals of the four forgers. The voltage measurements of the fully packaged handwriting signal acquisition device, consisting of four triboelectric sensors, were carried out using a multichannel oscilloscope. The commercial writing paper was placed on the device during actual testing, and people wrote characters on the commercial writing paper. The oscilloscope's four testing channels record the output voltage from the four triboelectric sensors and the written image was recorded on the writing paper simultaneously. The schematic diagram of the process for collecting handwriting signals using a triboelectric sensor array is shown in Figure 3A. The handwriting signals of the English character "Nature", Chinese character "自然", and numerical character "2022.03.24" by Mr. Liu (the genuine writer) are shown in Figure 3B–D, with the corresponding handwritten image information inserted in these figures. Figure 3E–G displays Miss Ma's representative traced handwriting signals of the English character "Nature", Chinese character "自然", and numerical character "2022.03.24", and with the corresponding traced handwritten images inserted in these figures. The representative traced handwriting signals of the English character "Nature", Chinese character "自然", and numerical

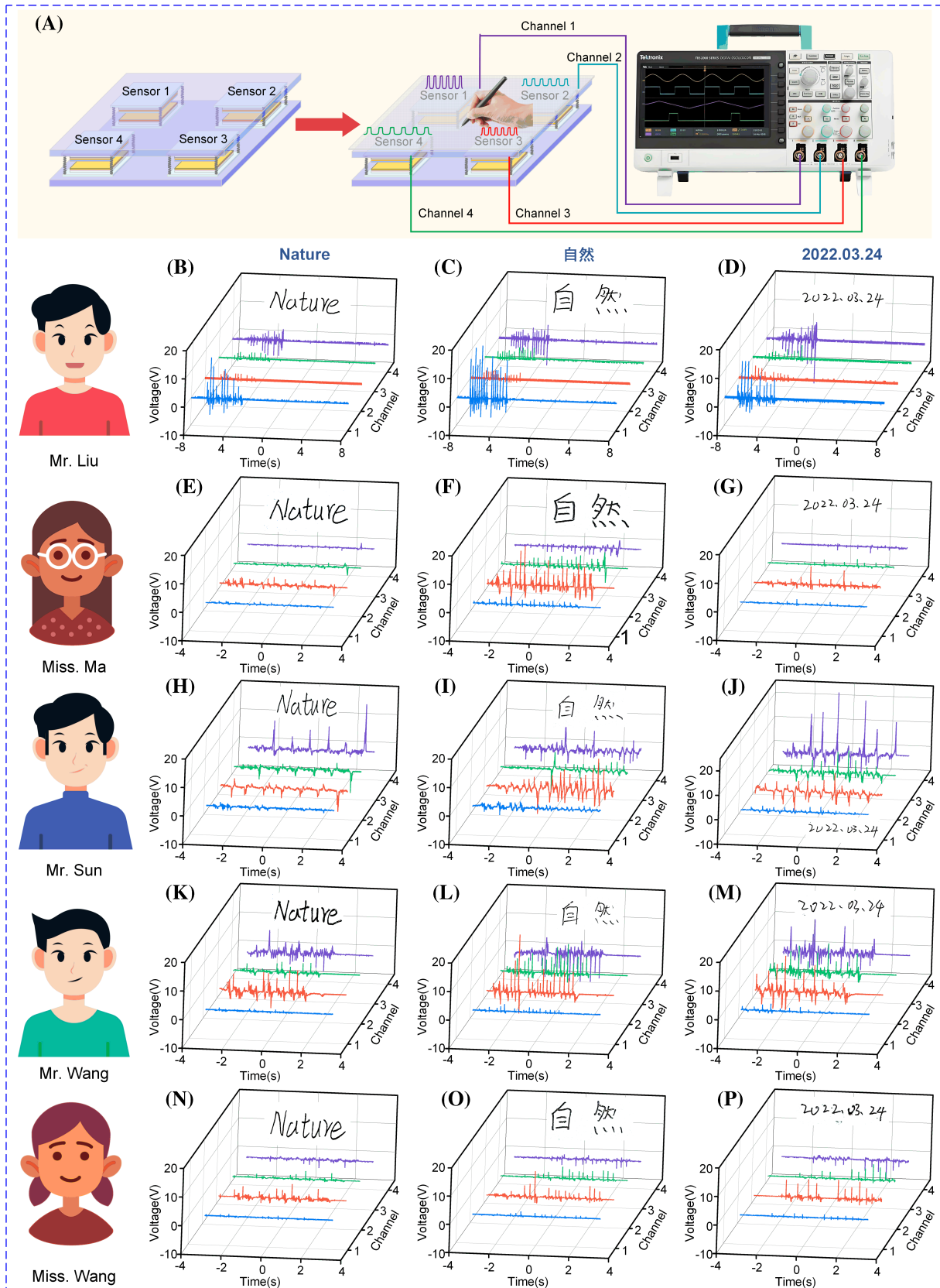


FIGURE 3 Legend on next page.

character “2022.03.24” by Mr. Sun are shown in Figure 3H–J, with the corresponding traced handwritten image information inserted in these figures. Similarly, Figure 3K–M exhibit Mr. Wang’s representative traced handwriting signals of the English character “Nature”, Chinese character “自然”, and numerical character “2022.03.24”, and with the corresponding traced handwritten images inserted in these figures. Figure 3N–P presents Miss Wang’s representative traced handwriting signals of the English character “Nature”, the Chinese character “自然”, and the numerical character “2022.03.24”, and with the corresponding traced handwritten images inserted in these figures. The four forgers had no prior practice or received professional training, and the forgers’ traced handwriting images and signals were obtained by tracing Mr. Liu’s handwriting image line-to-line. The forgers’ traced handwriting image is nearly identical to that of the genuine writer, as shown in the inserted images in Figure 3. Therefore, it is extremely challenging to conduct handwriting identification and verification based on the handwriting image. The handwriting signals were the time-series data and correlated to a variety of writing dynamic information, including the manner and rhythm of the writers’ habits, velocity, and applied writing force. Significant differences were observed in the handwriting signals between Mr. Liu and the four forgers when they wrote the same character, as demonstrated in Figure 3. Therefore, it is easy to distinguish forged handwriting from genuine handwriting based on the handwriting signals. Imitating is another common method for stealing signatures, where the handwriting of the genuine writer and the imitator both exhibit similar characteristics. The process of obtaining handwriting from the genuine writer and the forgers imitating the handwriting of the genuine writer was shown in Movie S2. The representative imitated handwriting signals of the English character “Nature”, Chinese character “自然”, and numerical character “2022.03.24” by the genuine writer and the four forgers were shown in Figure S4, with the corresponding traced handwritten images information inserted in these figures. Compared with traced handwriting, we observed differences between the imitated handwriting images of forgers and those of the genuine writer. The handwriting signals exhibit distinct variations. Similarly, while recognizing handwriting images poses certain difficulties, identifying

handwriting signals is much more straightforward. Figures S5 and S6 present representative samples of traced handwriting images and signals for all other characters utilized in this study. Figures S7–S15 show all the handwriting images of the genuine writer and the forgers’ traced handwriting images. Figures S16 and S17 present representative samples of imitated handwriting images and signals for all other characters utilized in this study. Figures S18–S26 show all the handwriting images of the genuine writer and the forgers’ imitated handwriting images.

2.4 | HWIS and recognition results

Here, a new machine learning architecture was developed to process the handwriting images and digital signals to identify the specific handwriting of the genuine writer. Obtaining abundant handwriting data from a genuine writer for model training was relatively easy, while acquiring handwriting data from forgers was challenging. To address this, we conceived the idea of effectively analyzing the intrinsic characteristics and extracting important features from the genuine writer’s handwriting data. By designing an intelligent one-class classifier that learns the inherent pattern properties of genuine handwriting, we can accurately identify the genuine writer’s handwriting and differentiate it from forgeries. This approach offers a suitable solution to the problem of handwriting identification. Consequently, an advanced deep learning architecture possessing powerful feature extraction capabilities and a one-class classification function was built. The architecture combines a mobile neural network, named MobileNetV2⁴⁶ with one-class support vector machine (OC-SVM) classifiers.⁴⁷ MobileNetV2 was utilized to extract exclusive handwriting habit features of the genuine writer, while OC-SVM learned the unique projection relation embedded in the genuine writer’s handwriting feature data. Since handwriting images and digital signals have different data formats, MobileNetV2 was designed to adapt to the corresponding format. For two-dimensional handwriting images, the convolutional calculations of MobileNetV2 were performed in two orthogonal directions,⁴⁸ while for one-dimensional signals, the convolutional calculations of MobileNetV2 were done in only one direction.⁴⁹ The difference led to the

FIGURE 3 Handwriting signals of English character “Nature”, Chinese character “自然”, and numerical character “2022.03.24”. (A) Schematic diagram of the process for collecting handwriting signals using a triboelectric sensor array. (B–D) Representative handwriting images and handwriting signals of Mr. Liu (genuine writer). (E–G) Miss Ma’s representative traced handwriting images and handwriting signals. (H–J) Mr. Sun’s representative traced handwriting images and handwriting signals. (K–M) Mr. Wang’s representative traced handwriting images and handwriting signals. (N–P) Miss Wang’s representative traced handwriting images and handwriting signals.

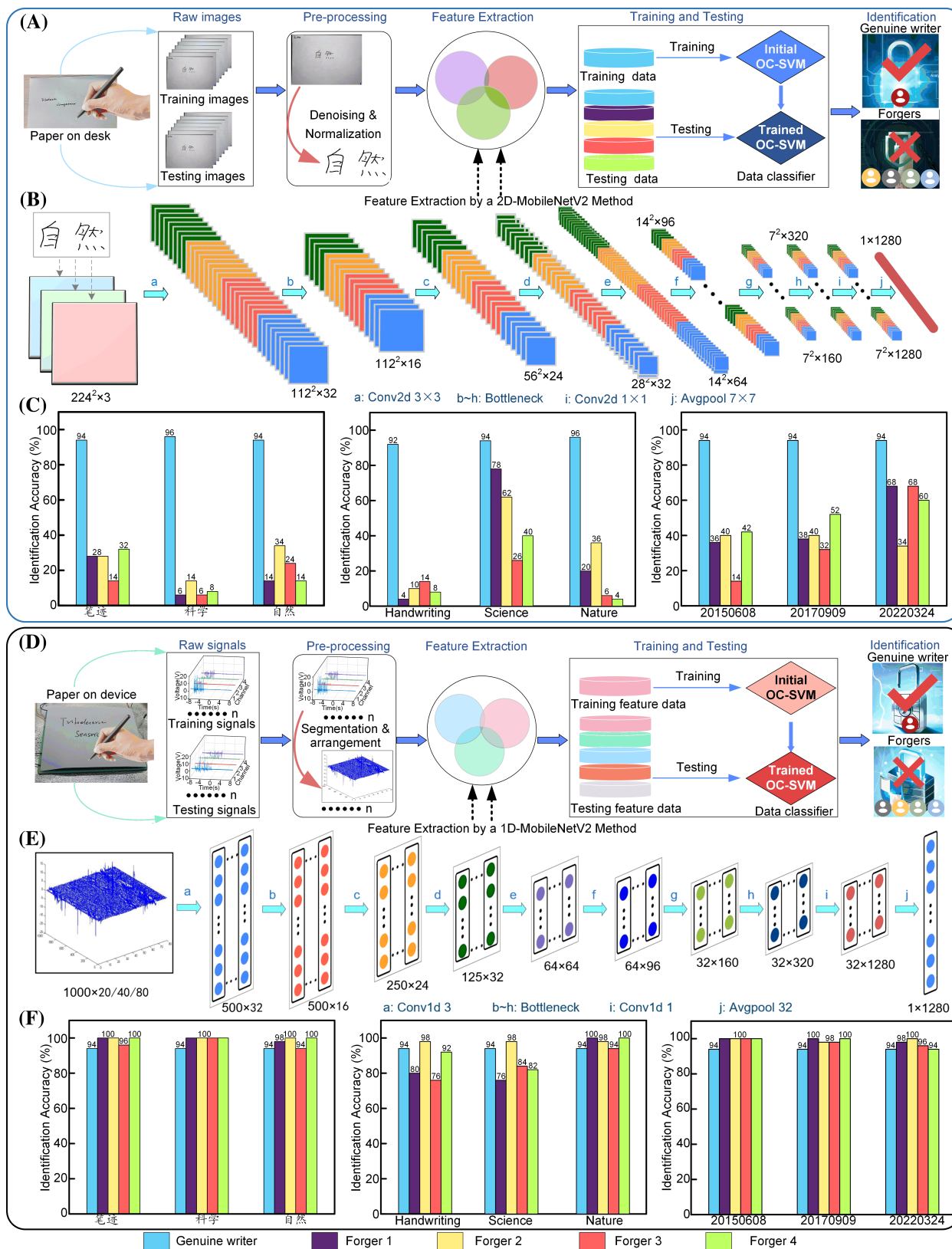


FIGURE 4 Legend on next page.

creation of two distinct MobileNetV2 models, which convert the handwriting images and digital signals into the same one-dimensional feature vectors as the inputs of OC-SVM, respectively. Thus, the disparity between the two handwriting recognition model architectures lies in the feature extraction process.

Figure 4 shows the proposed HWISs and the handwriting recognition results. The overall structure of the handwriting image identification system is depicted in Figure 4A. The handwriting image recognition workflow includes obtaining the handwriting images, preprocessing raw handwriting images, feature extraction, training and testing the machine learning model, and ultimately classifying and identifying handwriting images. Raw images were commonly affected by random noise and disturbances, so initial denoising and normalization were conducted to meet the basic input requirements of the two-dimensional MobileNetV2 (2D-MobileNetV2). Subsequently, the standardized images were input and processed through a pre-trained 2D-MobileNetV2 model. As shown in Figure 4B, the standardized images transform using a series of network layers, and the last layer of 2D-MobileNetV2 produces corresponding one-dimensional feature vectors, the number of which was the same as the number of the images. An OC-SVM classifier with default parameters was then employed to train these feature vectors, enabling the learning of the intrinsic correlation between these vectors and the genuine writer. Once the OC-SVM classifier had been appropriately trained, it was utilized to classify the handwriting feature vectors derived from both the genuine writer and forgers. To ensure the model's excellent performance in handwriting recognition, as many diverse characters as possible were used during model training. For instance, in recognizing Arabic numerals, the training samples selected as "2022.03.24", "2015.06.08", and "2017.09.09", which cover digits from 0 to 9. Figure 4C shows the handwriting image recognition results of the genuine writer and the traced handwriting image recognition results of the four forgers. The identification accuracies for the genuine writer's handwriting images of English, Chinese, and numerical characters were all over 94%, respectively. However, the identification accuracies of the four forgers' traced handwriting images of English characters, Chinese characters, and numerical characters ranged from 4% to 78%, and the vast majority of them were under an accuracy of 40%. This is because, upon careful examination of the

handwriting images, it becomes apparent that the traced handwriting images of forgers closely resemble the genuine handwriting of the actual writer. Compared with the traced handwriting images, there are some differences between the imitated handwriting and the genuine handwriting of the genuine writer. Similarly, utilizing the proposed handwriting image identification system for identifying, the recognition accuracies were not ideal, as shown in Figure S27A. Therefore, traditional image-based handwriting recognition methods were unable to effectively differentiate between the genuine handwriting of the genuine writer and the traced handwriting created by the forgers.

Figure 4D depicts the overall structure of the HWIS based on the handwriting signals acquired by the proposed triboelectric sensors array-enabled self-powered device. Similarly, the entire process involves handwriting signal acquisition, preprocessing the raw signals, extracting features, model training, testing, and identifying the handwriting signals. Raw handwriting signals typically consist of time-series data, so the initial step was to segment and rearrange the time-series handwriting signals to meet the input requirements of the one-dimensional MobileNetV2 (1D-MobileNetV2). Afterward, the standardized handwriting signals were input and processed through a pre-trained 1D-MobileNetV2 model. The details of the feature extraction processes are shown in Figure 4E. Subsequently, an OC-SVM classifier with default parameters was employed to train these feature vectors, allowing the learning of the intrinsic correlation between these vectors and the genuine writer. Once the OC-SVM classifier had been appropriately trained, it was employed to classify the handwriting feature vectors derived from both the genuine writer and forgers. Figure 4F shows the handwriting signal recognition results of the genuine writer and the traced handwriting signal recognition results of the four forgers. The handwriting identification accuracies of the genuine writer's English, Chinese, and numerical characters based on handwriting signals were all over 94%. The handwriting identification accuracies of the four forgers' handwriting signals of English, Chinese, and numerical characters by using handwriting signals by tracing the genuine writer's handwriting image ranged from 76% to 100%, with the majority exceeding 94%, as depicted in Figure 4E. Similarly, using our designed handwriting

FIGURE 4 HWIS and handwriting recognition results. (A) Overall structure of the handwriting image identification system. (B) Schematic diagram of the overall structure of the detailed 2D-MobileNetV2 model. (C) Identification accuracies of the genuine writer's handwriting images and forgers' imitated handwriting images of English, Chinese, and numerical characters. (D) Overall structure of the HWIS based on the handwriting signals. (E) Schematic diagram of the overall structure of the detailed 1D-MobileNetV2 model. (F) Identification accuracies of the genuine writer's handwriting and forgers' imitated handwriting of English, Chinese, and numerical characters based on the handwriting signals.

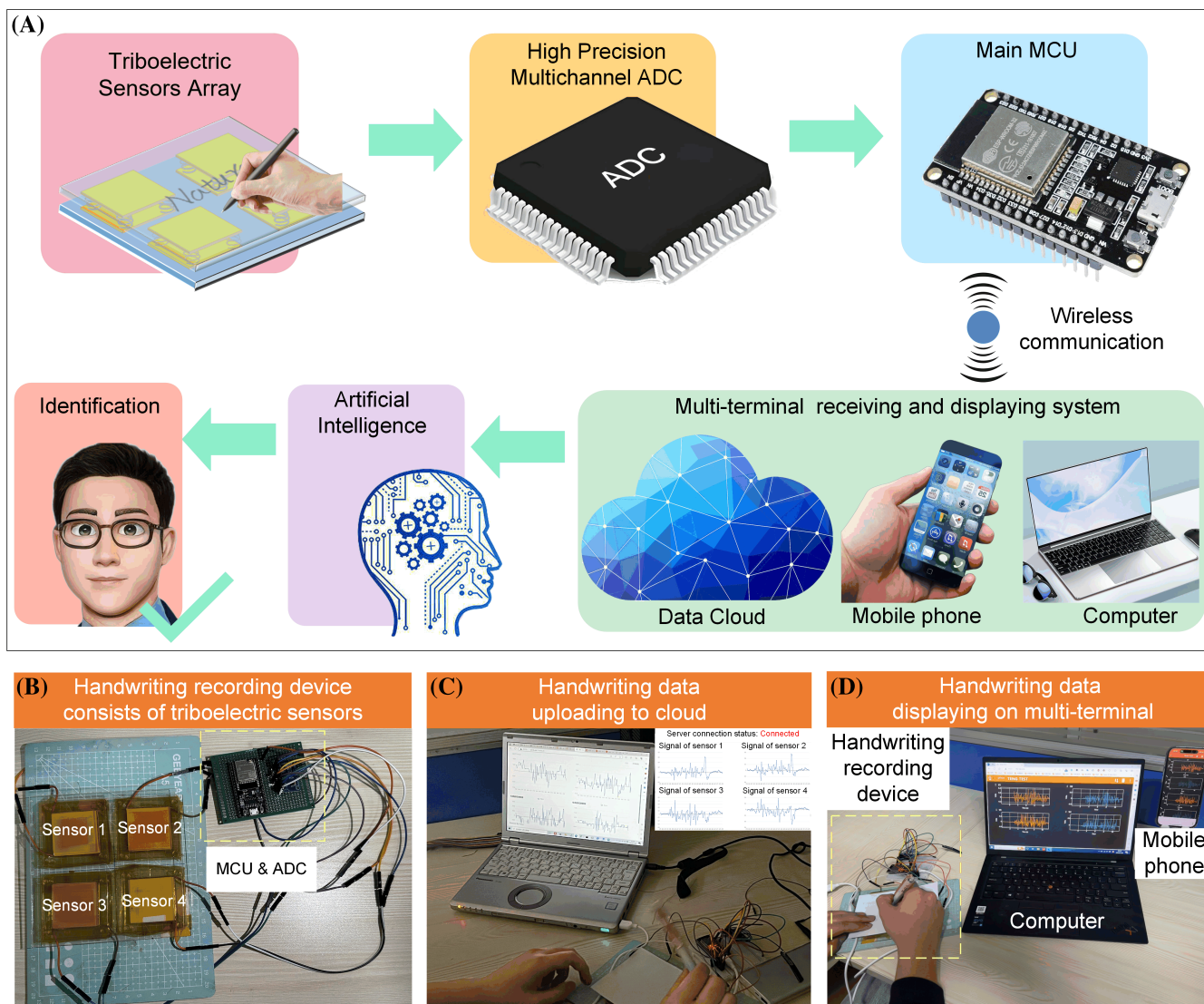


FIGURE 5 Demonstration of handwriting signals acquisition, wireless transmission, uploaded to a data cloud, and displayed on multi-terminals. (A) Flow chart of the system, including handwriting analog signals acquisition, processing/wireless transmission, artificial intelligence, and identification. (B) Photograph of the handwriting signals acquisition and wireless transmission system that consisted of a triboelectric sensors array. (C) Handwriting signals data uploaded to a data cloud. (D) Handwriting signals data wirelessly transmitted to multi-terminals and displayed.

recognition system based on handwriting signals to identify genuine writer's handwriting and forgers' imitated handwriting, the recognition accuracies were also quite high, as shown in Figure S27B. The designed triboelectric sensors array based self-powered device captured rich dynamic information during the process of forgers tracing the genuine writer's handwriting images to obtain traced handwriting. This suggested that the difference between the forgers' handwriting signals and the genuine writer's handwriting signals was much more pronounced than the difference between the forgers' traced/imitated handwriting images and the genuine writer's handwriting images. The recognition accuracies of handwriting signals were consistently higher than those of handwriting images, whether imitated or traced

handwriting of forgers. These findings indicated that the proposed HWIS, which incorporates the self-powered handwriting digital signal acquisition device based on triboelectric sensors and machine learning methods, holds the potential to solve the major challenge of handwriting identification and verification.

2.5 | Handwriting signal acquisition and wireless transmission system

For handwriting information, traditional methods involve recording the writer's strokes on paper and storing them physically, and in some cases, the handwritten images are scanned to create electronic versions for

digital storage. Figure 5A illustrates the proposed handwriting signal acquisition, wireless transmission, and recognition system flow chart. The handwriting signal recording device was based on a triboelectric sensor array to record handwriting information. Specifically, the device captures static image information of the handwriting on paper placed on the device, akin to the traditional method of recording and preserving handwritten information. More crucially, the system proposed in this study collected a wealth of dynamic handwriting information reflecting the writer's writing speed, pressure, and rhythm. Simultaneously, it displayed the dynamic handwriting signals during the writing process on multi-terminal devices, and access to detailed handwriting information was facilitated. Additionally, we have designed and implemented the capability to upload dynamic handwriting signal data to the data cloud, storing the handwriting information in a data cloud. This significantly enhanced data accessibility and security, making it convenient for users to back up and restore. In scenarios where handwriting recognition is needed, the proposed method of storing handwriting signal data in a data cloud allows users to download historical handwriting data from anywhere. By utilizing the well-trained artificial intelligence model, highly accurate recognition of the handwriting can be achieved. Figure 5B shows the photograph of the handwriting acquisition and wireless transmission systems that consisted of a triboelectric sensor array, a high-precision multichannel ADC chip, and a main MCU with wireless communication function. Benefits from this integrated design, the collection and wireless transmission of handwriting signals data have been achieved. When a person wrote characters on the paper placed on the device, the handwriting signal data was collected and uploaded to the data cloud, as shown in Figure 5C. The process of writing characters on the self-powered device, collecting handwriting signal data, wireless transmission, and uploading to a data cloud was shown in Movie S3. Based on the open-source phyphox software, we conducted secondary development to create our app. When a person writes on the paper that is placed on the developed device, thanks to the developed wireless transmission module, the handwriting signal data is wirelessly transmitted and displayed on the app installed on a smartphone or Pad. Additionally, remote access to the handwriting signal data can also be achieved on a computer through a web interface, as shown in Figure 5D. The process of writing characters on the self-powered device, collecting handwriting signal data, wireless transmission, and displaying them on multi-terminals was shown in Movie S4. This demonstration presents significant potential applications of the developed system in addressing the long-standing challenge of distinguishing between the genuine writer's signature

and the forgers' traced/imitated signature. Simultaneously, it enhances the security level of personal signatures and ensures the protection of private information.

3 | CONCLUSION

In summary, we developed a handwriting information data acquisition, wireless transmission, and identification system that consisted of the fully packaged triboelectric sensor array and machine learning methods. Thanks to the fully packaged method, these sensors demonstrated excellent resistance to humidity and dust. The developed system can capture both handwriting images and handwriting signal data. A mobile neural network called MobileNetV2 combined with a one-class support vector machine (OC-SVM) classifier was constructed for recognizing and identifying handwriting. We found that four forgers' traced handwriting images show virtually no differences compared with the genuine writer's handwriting image and the low recognition accuracies of handwriting images provide strong evidence. However, the developed system can capture rich dynamic handwriting information during the writing process, and the handwriting signal data of the genuine writer and forgers exhibit significant differences. The high recognition accuracies of handwriting signal data strongly demonstrated this conclusion. In a word, the recognition accuracies of handwriting signals were consistently higher than those of handwriting images, whether imitated or traced handwriting of forgers. We also showcased the physical implementation of the developed system, demonstrating its capabilities in handwriting signal data acquisition, wireless transmission, data uploading to the data cloud, and allocation on multiple display terminals. Additionally, we exhibited the system's capability for remote access and downloading the handwriting signal data through the data cloud, highlighting its practical value for fulfilling the requirements of handwriting recognition and identification applications. These findings indicated that the proposed HWIS holds significant potential to solve the major longstanding challenge of handwriting identification and verification that has perplexed humans for a considerable time. It can enhance the security level of personal signatures and ensure the protection of private information.

4 | EXPERIMENTAL SECTION

4.1 | Fabrication of triboelectric sensors

Fabrication of triboelectric sensors involves three main steps: triboelectric sensor fabrication, packaging, and assembly. For triboelectric sensor fabrication, FEP film

and Cooper film were used as the triboelectrification layer materials, copper as the electrode, PMMA as the support structure material, and EVA foam as a buffer layer to increase the contact area. In the case of the self-powered handwriting signal acquisition array device, which consisted of four triboelectric sensors, we cut the 125- μm thick FEP film into a 35×35 mm size and cleaned it sequentially in deionized water, alcohol, and deionized water baths using ultrasonic waves. A layer of conductive copper tape as the top electrode was attached to one surface of the FEP film. A piece of EVA foam with a size of $35 \times 35 \times 3$ mm was then attached to the top electrode, followed by attaching a $35 \times 35 \times 1$ mm PMMA piece to the EVA foam. The FEP-EVA-PMMA sandwich structure was attached to a $50 \times 50 \times 1$ mm PMMA piece using a double-faced adhesive tape, with the PMMA faces facing each other, thus completing the upper part of a TENG. For the lower part of the triboelectric sensor, a layer of conductive copper tape was attached to the top surface of a $35 \times 35 \times 3$ mm EVA foam piece. The EVA foam was then attached to the surface of a $35 \times 35 \times 1$ mm PMMA piece. The EVA foam with a copper layer was attached to a $50 \times 50 \times 1$ mm PMMA piece using double-faced adhesive tape, with the EVA foam facing the PMMA, completing the lower part of the triboelectric sensor. Finally, the upper and lower parts were assembled by fixing four springs at each angle of a $50 \times 50 \times 1$ mm PMMA piece, resulting in the fabrication of a complete triboelectric sensor. Following triboelectric sensor fabrication, we proceeded with the packing processes. In this work, a layer of Kapton film was used to package the triboelectric sensor to eliminate the effect of environmental humidity and dust on the electrical output performance of the device. Ultimately, four fully packaged triboelectric sensors were fabricated using the above process and attached to a piece of PMMA with a size of $120 \times 120 \times 1.5$ mm, which served as the top panel. A writing pad with a size of $148 \times 210 \times 2$ mm was then attached to the underside of the four triboelectric sensors, creating a self-powered handwriting signal recording device.

4.2 | Characterization and measurements

For characterizing the electrical output performance of the contact-separation mode triboelectric sensor, a linear motor was used to drive the sensor contact and separate periodically. A high-voltage source meter was used to electrify the FEP. To ensure consistent experimental conditions, a force sensor (HYchangan, HYMH-019) was

utilized to measure the force in real-time. A humidity meter (DRETEC, O-230) was employed to measure the humidity of the experimental condition. A programmable electrometer (Keithley, 6517B) was used to measure the open-circuit voltage, short-circuit current, and transfer charges. The voltage measurements of the fully packaged handwriting signal acquisition device that consisted of four triboelectric sensors were carried out using a multichannel oscilloscope (Tektronix, TBS2104B) with the normal probe 10 M Ω .

4.3 | Handwriting dataset collection

Regarding the handwriting dataset, we aimed to demonstrate the generality and excellence of the proposed HWIS in identifying various character types commonly encountered in our daily work and life, including Chinese, English, and numerical characters. The Chinese phrases “自然”, “学科”, “笔迹”, their corresponding English translations, “Nature”, “Science”, and “Handwriting”, as well as three numerical combinations, “2015.06.08”, “2017.09.09”, and “2022.03.24”, were selected as textual samples for our research. To collect the handwriting images and digital signals from both the genuine writer and forgers, we recruited five undergraduate students as volunteers. Mr. Liu, as the genuine writer, wrote the selected characters on the commercially available paper fixed on the self-powered handwriting digital signal acquisition device, repeating this process 50 times for each character. We recorded his handwriting images on paper while capturing the handwriting digital signals using the device. The four forgers, using both imitating and tracing methods, wrote the selected characters on the commercially available paper fixed to the device. Again, the process was repeated 50 times for each selected character. As a result, we simultaneously obtained 50 imitated and traced handwriting images and digital signals.

4.4 | Demonstration of the system application

For the real-time demonstration of the system, the triboelectric sensors array connects to a four-channel high-precision ADC, ensuring that each triboelectric sensor is connected to the appropriate channel to capture its analog signal. Connect the pins of the four-channel high-precision ADC to the corresponding pins of an ESP32 microcontroller to receive the signal output from the ADC. A filtering algorithm is programmed on the ESP32 microcontroller to filter the signal collected from the

ADC. A program was written to transmit handwriting signal data, using Bluetooth wireless transmission protocol to a specified receiver. At the receiving terminal, perform secondary development of the open-source phyphox software to receive data from the ESP32 microcontroller and achieve real-time display. The ESP32 establishes internet communication via WiFi, connecting to the server using the WebSocket protocol. It sends four sets of data to the server in the form of a JSON array for processing. The processed data is then displayed using a web page written with Vue.js and Chart.js, allowing for the simultaneous visualization of data from four channels.

ACKNOWLEDGMENTS

This work was supported by the National Natural Science Foundation of China (Grant Nos. 52105206, 62241308, and 92271201), Guangdong Basic and Applied Basic Research Foundation (2023A1515240050), China Postdoctoral Science Foundation (Grant No. BX2021230), and the Opening Project of National and local joint Engineering Research Center for industrial friction and lubrication technology (Grant No. 2023-GD-0001). We also thank Mingxin Liu, Yingqiao Wang, Yuning Ma, Shihao Wang, and Yakai Sun for their volunteer work in the experiment and for their agreement to demonstrate handwriting signal data gathering and the use of their photos in the work. No formal approval for the experiments involving human volunteers was required. The volunteers took part following informed consent.

CONFLICT OF INTEREST STATEMENT

The authors declare no conflict of interest.

ORCID

Zhong Lin Wang  <https://orcid.org/0000-0002-5530-0380>

REFERENCES

- Feng H, Wah C. Private key generation from on-line handwritten signatures. *Inf Manage Comput Secur*. 2002;10(4):159-164.
- Tapiador M, Gómez J, Sigüenza JA. *Writer identification forensic system based on support vector machines with connected components[C]//International Conference on Industrial, Engineering and Other Applications of Applied Intelligent Systems*. Springer Berlin Heidelberg; 2004:625-632.
- Fornés A, Lladós J, Sánchez G, Bunke H. On the use of textural features for writer identification in old handwritten music scores. *2009 10th International Conference on Document Analysis and Recognition (ICDAR'10)*. IEEE; 2009:996-1000.
- Awaida S, Mahmoud S. Writer identification of arabic text using statistical and structure features. *Cybernet Syst*. 2013; 44(1):57-76.
- Liu X, Lian Y. Handwriting identification: challenges and solutions. *J Forensic Sci Med*. 2018;4(3):167-173.
- Chaudhari K, Thakka A. Survey on handwriting-based personality trait identification. *Expert Syst Appl*. 2019;124:282-308.
- Chahi A, Khadiri I, Merabet Y, Ruichek Y, Touahni R. Block wise local binary count for off-line text-independent writer identification. *Expert Syst Appl*. 2018;93:1-14.
- Mushtaq F, Mishar M, Kumar M, Khurana S. UrduDeepNet: offline handwritten urdu character recognition using deep neural network. *Neural Comput Appl*. 2021;33(22):15229-15252.
- Xue G, Liu S, Gong D, Ma Y. APT-DenseNet: a hybrid deep learning-based gender identification of handwriting. *Neural Comput Appl*. 2021;33:4611-4622.
- Guo H, Wang J, Wang H, et al. Self-powered intelligent human-machine interaction for handwriting recognition. *Research*. 2021;2021:4689869.
- Hadjadi B, Chibani Y. Two combination stages of clustered one-class classifiers for writer identification from text Fragmentsm. *Pattern Recogn*. 2018;82:147-162.
- Tcho IW, Kim WG, Choi YK. A self-powered character recognition device based on a triboelectric nanogenerator. *Nano Energy*. 2020;70:104534.
- Cao V, Kim M, Lee S, et al. Chemically modified MXene nanoflakes for enhancing the output performance of triboelectric nanogenerators. *Nano Energy*. 2023;107:108128.
- Kim M, Park D, Alam M, Lee S, Park P, Nah J. Remarkable output power density enhancement of triboelectric nanogenerators via polarized ferroelectric polymers and bulk MoS₂ composites. *ACS Nano*. 2019;13(4):4640-4646.
- Jin T, Sun Z, Li L, et al. Triboelectric nanogenerator sensors for soft robotics aiming at digital twin applications. *Nat Commun*. 2020;11(1):5381.
- Guo H, Pu X, Chen J, et al. A highly sensitive, self-powered triboelectric auditory sensor for social robotics and hearing aids. *Sci Robot*. 2018;3(20):eaat2516.
- Liu Y, Liu W, Wang Z, et al. Quantifying contact status and the air-breakdown model of charge-excitation triboelectric nanogenerators to maximize charge density. *Nat Commun*. 2020;11(1):1599.
- Wang Z, Liu W, He W, et al. Ultrahigh electricity generation from low-frequency mechanical energy by efficient energy management. *Joule*. 2021;5(2):441-455.
- Lee D, Rubab N, Hyun I, et al. Ultrasound-mediated triboelectric nanogenerator for powering on-demand transient electronics. *Sci Adv*. 2022;8(1):eab18423.
- Kim WG, Kim DW, Tcho IW, Kim JK, Kim MS, Choi YK. Triboelectric nanogenerator: structure, mechanism, and applications. *ACS Nano*. 2021;15(1):258-287.
- Zhang W, Diao D, Sun K, Fan X, Wang P. Study on friction-electrification coupling in sliding-mode triboelectric nanogenerator. *Nano Energy*. 2018;48:456-463.
- Xu W, Zheng H, Liu Y, et al. A droplet-based electricity generator with high instantaneous power density. *Nature*. 2020; 578(7795):392-396.
- Yang D, Guo H, Chen X, et al. A flexible and wide pressure range triboelectric sensor array for real-time pressure detection and distribution mapping. *J Mater Chem A*. 2020;8(45):23827-23833.

24. Lu Y, Tian H, Cheng J, et al. Decoding lip language using triboelectric sensors with deep learning. *Nat Commun.* 2022;13(1):1-12.
25. Su Y, Chen G, Chen C, et al. Self-powered respiration monitoring enabled by a triboelectric nanogenerator. *Adv Mater.* 2021;33(35):2101262.
26. Xie X, Wen Z, Shen Q, et al. Impedance matching effect between a triboelectric nanogenerator and a piezoresistive pressure sensor induced self-powered weighing. *Adv Mater.* 2018;3(6):1800054.
27. Chen C, Chen L, Wu Z, et al. 3D double-faced interlock fabric triboelectric nanogenerator for bio-motion energy harvesting and As self-powered stretching and 3D tactile sensors. *Mater Today.* 2020;32:84-93.
28. Zhang X, Yu Y, Xia X, et al. Multi-mode vibrational triboelectric nanogenerator for broadband energy harvesting and utilization in smart transmission lines. *Adv Energy Mater.* 2023;13(43):2302353.
29. Fang L, Zheng Q, Hou W, Zheng L, Li H. A self-powered vibration sensor based on the coupling of triboelectric nanogenerator and electromagnetic generator. *Nano Energy.* 2022;97:107164.
30. Chen J, Pu X, Guo H, et al. A self-powered 2D barcode recognition system based on sliding mode triboelectric nanogenerator for personal identification. *Nano Energy.* 2018;43:253-258.
31. Guo H, Jia X, Liu L, Cao X, Wang N, Wang ZL. Freestanding triboelectric nanogenerator enables noncontact motion-tracking and positioning. *ACS Nano.* 2018;12(4):3461-3467.
32. Chen B, Tang W, Wang Z. Lm advanced 3D printing-based triboelectric nanogenerator for mechanical energy harvesting and self-powered sensing. *Mater Today.* 2021;50:224-238.
33. Zhang W, Deng L, Yang L, et al. Multilanguage-handwriting self-powered recognition based on triboelectric nanogenerator enabled machine learning. *Nano Energy.* 2020;77:105174.
34. Guo H, Wan J, Wu H, et al. Self-powered multifunctional electronic skin for a smart anti-counterfeiting signature system. *ACS Appl Mater Int.* 2020;12(19):22357-22364.
35. Xiang S, Tang J, Yang L, Guo Y, Zhao Z, Zhang W. Deep learning-enabled real-time personal handwriting electronic skin with dynamic thermoregulating ability. *NPJ Flex Electron.* 2022;6(1):59.
36. Wen R, Guo J, Yu A, Zhai J, Wang ZL. Humidity-resistive triboelectric nanogenerator fabricated using metal organic framework composite. *Adv Funct Mater.* 2019;29(20):1807655.
37. Zhou Q, Lee K, Kim KN, et al. High humidity-and contamination-resistant triboelectric nanogenerator with superhydrophobic interface. *Nano Energy.* 2019;57:903-910.
38. Chen X, Champod C, Yang X, et al. Assessment of signature handwriting evidence via score-based likelihood ratio based on comparative measurement of relevant dynamic features. *Forensic Sci Int.* 2018;282:101-110.
39. Mohammed L, Found B, Caligiuti M, Rogers D. Dynamic characteristics of signatures: effects of writer style on genuine and simulated signature. *J Forensic Sci.* 2015;60(1):89-94.
40. Wen F, Zhang Z, He T, Lee C. AI enabled sign language recognition and VR space bidirectional communication using triboelectric smart glove. *Nat Commun.* 2021;12(1):5378.
41. Shi Y, Yang P, Lei R, et al. Eye tracking and eye expression decoding based on transparent, flexible and ultra-persistent electrostatic interface. *Nat Commun.* 2023;14(1):3315.
42. Zhou Z, Chen K, Li X, et al. Sign-to-speech translation using machine-learning-assisted stretchable sensor arrays. *Nat Electron.* 2020;3(9):571-578.
43. Jiao P, Wang ZL, Alavi AH. Maximizing triboelectric nanogenerators by physics-informed AI inverse design. *Adv Mater.* 2024;36(5):2308505.
44. Sun Z, Zhu M, Shan X, Lee C. Augmented tactile-perception and haptic-feedback rings As human-machine interfaces aiming for immersive interactions. *Nat Commun.* 2022;13(1):5224.
45. Zhu J, Ji S, Ren Z, et al. Triboelectric-induced ion mobility for artificial intelligence-enhanced mid-infrared gas spectroscopy. *Nat Commun.* 2023;14(1):2524.
46. Sandler M, Howard A, Zhu M, Zhmoginov A, Chen L. MobileNetV2: inverted residuals and linear bottlenecks. *2018 IEEE/CVF Conference on Computer Vision and Pattern Recognition (CVPR 2018).* IEEE; 2018:4510-4520.
47. Xing H, He Z. Adaptive loss function based least squares one-class support vector machine. *Pattern Recogn Lett.* 2022;156:174-182.
48. Arslan Ö. Automated detection of heat valve disorders with time-frequency and deep features on PCG signals. *Biomed Signal Process.* 2022;78:103929.
49. Sattarifar A, Nestorović T. Damage localization and characterization using one-dimensional convolutional neural network and a sparse network of transducers. *Eng Appl Artif Intel.* 2022;115:105273.

SUPPORTING INFORMATION

Additional supporting information can be found online in the Supporting Information section at the end of this article.

How to cite this article: Zhang W, Deng L, Lü X, et al. Advanced handwriting identification: Triboelectric sensor array integrating with deep learning toward high information security. *InfoMat.* 2025;e70002. doi:[10.1002/inf2.70002](https://doi.org/10.1002/inf2.70002)